GEOLOGY | THE GEOLOGICAL SOCIETY OF AMERICA®

https://doi.org/10.1130/G47778.1

Manuscript received 20 April 2020
Revised manuscript received 30 June 2020
Manuscript accepted 5 July 2020

Syncing fault rock clocks: Direct comparison of U-Pb carbonate and K-Ar illite fault dating methods

C.M. Mottram[1]*, D.A. Kellett[2], T. Barresi[3], H. Zwingmann[4], M. Friend[5], A. Todd[6] and J.B. Percival[7]

[1]School of the Environment, Geography and Geosciences, University of Portsmouth, Portsmouth PO1 3QL, UK
[2]Geological Survey of Canada, Dartmouth, Nova Scotia B2Y 4A2, Canada
[3]Triumph Gold Corporation, Vancouver, British Columbia V6E 3V6, Canada
[4]Department of Geology and Mineralogy, University of Kyoto, Kyoto 606-8501, Japan
[5]Department of Earth, Ocean and Atmospheric Sciences, University of British Columbia, Vancouver, British Columbia V6 T 1Z4, Canada
[6]CSIRO Energy, Perth, Western Australia 6152, Australia
[7]Geological Survey of Canada, Ottawa, Ontario K1A 0E8, Canada

ABSTRACT

The timing of slip on brittle faults in Earth's upper crust is difficult to constrain, and direct radiometric dating of fault-generated materials is the most explicit approach. Here we make a direct comparison between K-Ar dating of fault gouge clay (authigenic illite) and U-Pb dating of carbonate slickenfibers and veins from the same fault. We have dated fault generated materials from the Big Creek fault, a northwest-striking, dextral strike-slip fault system in Yukon Territory, Canadian Cordillera. Both methods yielded dates at ca. 73 Ma and ca. 60–57 Ma, representing at least two periods of fault slip that form part of a complex fault and fluid-flow history. The Cretaceous result lies within previous indirect estimates for major slip on the fault. The Paleocene–Eocene result coincides with the estimated timing of slip of the nearby Tintina and Denali faults, which are crustal-scale, northwest-striking dextral faults, indicating Big Creek fault reactivation during regional faulting. The coincidence of periods of carbonate-crystallizing fracturing and fluid flow with intervals of seismic, gouge-generating slip supports the fault valve model, where fault strength is mediated by fluid pressures, and fluid emplacement requires seismic pumping in otherwise impermeable aseismic fault zones. The reproducibility of slip periods for distinct fault-generated materials using different decay systems indicates that these methods provide complimentary results and can be reliably applied to date brittle fault slip, opening new opportunities for investigating fault conditions with associated mineralizing fluid events.

DATING BRITTLE FAULTS

Brittle faults record past seismic slip events and are major fluid conduits, channeling magma, ore-generating fluids, oil, gas, and water (Haines et al., 2016). In the fault valve model, fluids mediate fault strength, acting as a catalyst for seismic slip (Sibson, 1992). Determining periods of frictional slip and fault-related fluid flow is critical for testing fault strength models. Fault histories are also important for building regional tectonic frameworks, understanding ore genesis, forming basin evolution models, and studying seismically active faults that pose geohazards and engineering challenges (e.g., Zwingmann et al., 2010). Fault timing is typically constrained through cross-cutting relationships, but is more precisely achieved by direct dating of fault-generated materials such as fault gouge, slip-surface hematite, opal, pseudotachylyte, and slickenfibers (Nuriel et al., 2012, 2019a; Tagami, 2012; Ault et al., 2015; Tillberg et al., 2020).

Potassium-argon (K-Ar) and/or $^{40}Ar/^{39}Ar$ dating of authigenic illite, a K-rich clay mineral that forms instantaneously during faulting, is a common method for fault dating (van der Pluijm et al., 2001; Vrolijk et al., 2018; Tsukamoto et al., 2019). However, the potential for wall-rock inheritance and multiple clay-generating slip events generally results in a positive correlation between K-Ar illite age and clay grain size (e.g., Torgersen et al., 2015a, 2015b), which can be challenging to deconvolve.

Carbonate U-Pb geochronology can provide direct timing constraints for geological processes including diagenesis, fluid flow, and tectonic processes (e.g., Rasbury and Cole, 2009). *In situ* U-Pb dating has been applied to low-U fault-related carbonate (e.g., Roberts and Walker, 2016; Nuriel et al., 2017; Parrish et al., 2018; Roberts et al., 2020). Previous indirect comparison of fault-gouge illite $^{40}Ar/^{39}Ar$ and carbonate U-Pb ages suggests concordance between the two methods (Nuriel et al., 2019b), but no direct comparison has been undertaken by applying both techniques to colocated samples from the same fault system. Here we test the hypothesis that fault-gouge illite and fault-related carbonate provide corresponding records of fault slip through direct comparison of K-Ar fault-gouge illite and U-Pb carbonate ages from a single fault system. Our study area lies within a copper-gold porphyry district where fault slip history is critical for developing the metallogenic framework for the region.

BIG CREEK FAULT

The Big Creek fault is a >150-km-long, northwest-southeast–striking, dextral strike-slip fault network located in the Yukon Territory, Canada (Fig. 1), between and subparallel to the Denali and Tintina dextral strike-slip faults (>350 km and ~440 km of Paleogene displacement, respectively; Lanphere, 1978; Hayward, 2015). The Big Creek fault cuts the metamorphosed Paleozoic Yukon-Tanana terrane, one of several terranes accreted to Laurentia during the early Mesozoic to form the Canadian Cordillera (Colpron et al., 2006). Intrusive units within the Yukon-Tanana terrane include the Jurassic Long Lake (ca. 192–178 Ma) and the Cretaceous

*E-mail: catherine.mottram@port.ac.uk

CITATION: Mottram, C.M., et al., 2020, Syncing fault rock clocks: Direct comparison of U-Pb carbonate and K-Ar illite fault dating methods: Geology, v. 48, p. , https://doi.org/10.1130/G47778.1

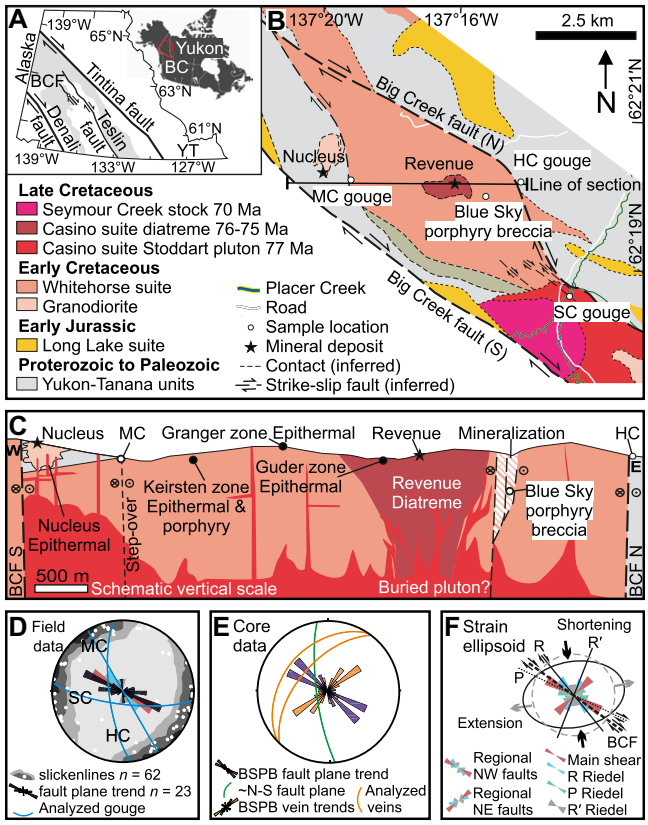

Figure 1. (A) Yukon Territory, Canada, showing key structures (BC—British Columbia; BCF—Big Creek fault; YT—Yukon Territory). (B) Regional map of Big Creek fault, after Allan and Friend (2018) (sample sites: MC—Mechanic Creek; HC—Happy Creek; SC—Seymour Creek). (C) Schematic cross section (see B for location) including major faults and mineral deposits. (D) Stereonet of field data, including slickenlines (contoured line data at 2° intervals), fault planes (rose diagram of plane trends), and great circles of gouge zones. (E) Stereonet of Blue Sky porphyry breccia (BSPB) core data including rose diagrams of fault plane and vein trends. Great circles are of analyzed carbonate veins. (F) Strain ellipsoid for Big Creek fault, adapted from Sánchez et al., (2014).

Whitehorse (ca. 112–105 Ma) and Casino (ca. 79–72 Ma) suites (Allan et al., 2013; Colpron et al., 2016; Friend et al., 2017; Fig. 1). A suite of extrusive rocks was emplaced ca. 72–67 Ma, including the Carmacks Group volcanic rocks (Allan et al., 2013). Both intrusive Cretaceous suites are associated with Cu-Au porphyry and related deposits that are aligned and spatially associated with the Big Creek fault (Johnston, 1999), including the Nucleus and Revenue deposits, which lie within a releasing bend between the main fault strands (Fig. 1; Allan et al., 2013).

Regional mapping and geochronology provide a framework for Big Creek fault slip (Fig. 1; Friend et al., 2017; Allan and Friend, 2018). The ca. 77 Ma Stoddart pluton is interpreted to plug the northern fault strand, providing a minimum age for slip. The 70 Ma Seymour Creek stock is truncated by the southern fault strand, providing a maximum age for slip. Thus, there were at least three apparent slip periods: (1) structurally controlling emplacement of the Whitehorse suite ca. 112–105 Ma, (2) slip coeval with emplacement of the Casino suite and associated mineralization during 79–72 Ma, and (3) slip after 70 Ma (Allan et al., 2013; Friend et al., 2017).

FAULT-GENERATED MATERIALS

The Big Creek fault crops out in a few meter-scale fractured outcrops, where slickenlines and fault planes follow the regional northwest-southeast trend (Fig. 1D). We sampled freshly exposed fault gouge from three newly dug trenches: Seymour Creek (SC), Mechanic Creek (MC), and Happy Creek (HC; Figs. 1 and 2; precise locations are listed in the Supplemental Material[1]). SC gouge was sampled from a 20-cm-wide, clay-rich seam oriented 097°/75° (strike/dip) within fractured and altered Stoddart pluton monzonite (ca. 77 Ma; Allan and Friend, 2018). MC gouge was sampled from a 150°-trending, 5-m-wide subvertical gouge zone bounded by silica-altered wall rock of 107 ± 1 Ma Whitehorse suite granodiorite (Friend et al., 2017). HC gouge was sampled from a 20-cm-wide gouge zone oriented ~173/74° and hosted in Paleozoic layered schist.

The 6-km-long mineralized trend that hosts the Revenue-Nucleus Au-Ag-Cu-Mo deposits is contained mainly within Whitehorse suite granodiorite and surrounding Yukon-Tanana terrane (Fig. 1C). The deposits are interpreted to be high-level expressions of a porphyry system (Friend et al., 2017). Mineralization is thought to be related to magmatic fluids associated with the Late Cretaceous intrusive bodies. Steeply inclined hydrothermal breccia pipes, e.g., the Blue Sky porphyry breccia (BSPB), are interpreted to be emplaced along the margins of rotated blocks within the Big

[1]Supplemental Material. Full analytical materials, gouge and detailed carbonate sample descriptions and locations, summary of additional U-Pb geochronology plots and interpretation, structural data, and Data Set S1 (K-Ar results), Data Set S2 (X-ray diffraction results), Data Set S3 (U-Pb carbonate results), and Data Set S4 (U-Pb standard reproducibility). Please visit https://doi.org/10.1130/GEOL.S.12730811 to access the supplemental material, and contact editing@geosociety.org with any questions.

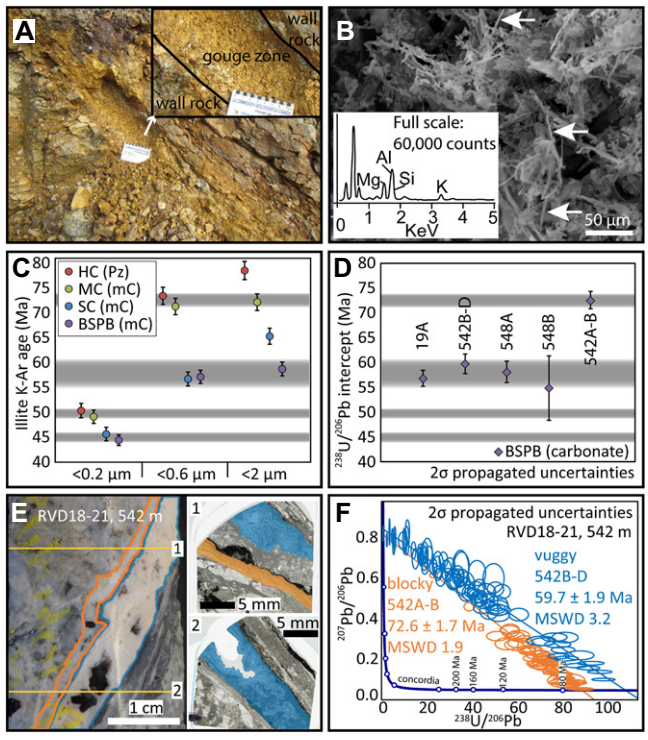

Figure 2. (A) Seymour Creek (SC, Yukon Territory, Canadian Cordillera) fault-gouge sample site; view toward the southeast. Scale is in centimeters. (B) Scanning electron microcopy secondary electron image with inset energy dispersive spectra of <0.2 µm Mechanic Creek (MC) gouge; fibrous authigenic illite particles are shown by arrows. (C) K-Ar age versus illite grain size, with interpreted fault events shown by gray bars. HC—Happy Creek; BSPB—Blue Sky porphyry breccia; Pz—Paleozoic wall rocks; mC—mid-Cretaceous wall rocks. (D) U-Pb carbonate dates, labeled with sample numbers. (E) Sample RVD18-21, 542 m core depth hand specimen and two analyzed sections showing blocky (orange) and vuggy (blue) carbonate. (F) U-Pb carbonate Tera-Wasserburg plot of sample RVD18-21, 542 m core depth (MSWD—squared weighted deviation).

Creek fault releasing bend that are structurally-controlled by approximately north-south– and northwest-southeast–striking, subvertical faults (Figs. 1C, 1E). Samples (all quoted as core depth in meters) collected from the BSPB drill core include carbonate slickenfibers from core RVD18-19 (314 m) and mineralized carbonate veins oriented ~239°/73° from core RVD18-21 (542 m and 548 m) (Fig. 1E; ~90° to faults in the same core). Veins are characterized as (1) ~1-mm-thick blocky carbonate with pyrite margins, and (2) ~1–10-mm-thick vuggy carbonate with chalcopyrite, pyrite, and barite inclusions. Approximately north-south–striking fault gouge was collected from core RVD18-21 (557) m (Fig. 2; see the Supplemental Material).

METHODS AND RESULTS

Fault gouge samples were separated via ultra-centrifugation to isolate clay-sized fractions 2.0–0.6, 0.6–0.2, and <0.2 µm, which were then characterized using X-ray diffraction and imaged using a scanning electron microscope (Fig. 2). The analytical method used for K-Ar dating is described in Zwingmann and Mancktelow (2004). Ages are reported at 2σ (see the Supplemental Material and Data Set S1 for the full methods and results). Gouge samples contain ~25% (HC) to ~100% (MC) illite. No other K-bearing phases are present except ~2% K-feldspar in the 2–0.6 µm fraction of HC Data Set S2). Gouge ages range from ca. 79 Ma to 44 Ma, with common ages for MC and HC gouge, and for SC and BSPB gouge (Fig. 2; Table 1).

Carbonate slickenfibers and veins were characterized under plane-polarized light. Suitable domains with high U (~<1–10 ppm) and low Pb were identified with spot analyses. U-Pb isotopic analysis was conducted using laser ablation–inductively coupled plasma–mass spectrometry (LA-ICP-MS), as described in Parrish et al. (2018; Supplemental Material and Data Set S4). Analyses of seven carbonate polished sections yielded U-Pb ages of ca. 73 and 60–57 Ma (Table 1; Fig. 2; Data Set S3).

TABLE 1. GEOCHRONOLOGY RESULTS

K-Ar Illite Data			
Sample	Grain size (µm)	K-Ar age (Ma)	Error (2σ; Ma)
Mechanic Creek (MC)	2–0.6	72.2	1.7
	0.6–0.2	71.3	1.7
	<0.2	49.1	1.3
Happy Creek (HC)	2–0.6	78.6	1.8
	0.6–0.2	73.4	1.7
	<0.2	50.4	1.5
Seymour Creek (SC)	2–0.6	65.3	1.6
	0.6–0.2	56.8	1.4
	<0.2	45.7	1.4
Blue Sky porphyry breccia (BSPB) sample RVD18–21, 557 m	2–0.6	58.7	1.4
	0.6–0.2	57.2	1.3
	<0.2	44.4	1.1

U-Pb Carbonate Data			
Sample (all BSPB)	$^{238}U/^{206}Pb$ age* (Ma)	Uncertainty (2σ; Ma)	MSWD, *n*
RVD18-21, 542 m			
Sections A–B, blocky	72.6	1.7	MSWD = 1.9, *n* = 54
Sections B-D, vuggy	59.7	1.9	MSWD = 3.2, *n* = 84
RVD18-21, 548 m			
Section A, vuggy	58.1	2.1	MSWD = 1.9, *n* = 44
Section B, vuggy	54.8	6.5	MSWD = 3.7, *n* = 29
RVD18-19, 314 m			
Section A, slickenfiber	56.8	1.7	MSWD = 2.6, *n* = 42

*$^{238}U/^{206}Pb$ intercept age.

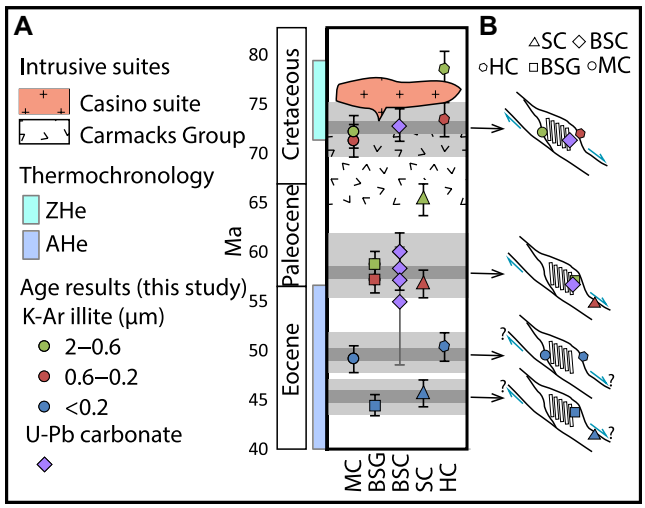

Figure 3. (A) Summary of fault slip history for Big Creek fault (Yukon Territory, Canadian Cordillera). Zircon (U-Th)/He (ZHe) and apatite (U-Th)/He (AHe) age ranges indicate when area cooled below ~180 °C and ~60 °C, respectively, from Bineli Betsi et al. (2012). Error bars are 2σ. Gray bars indicate interpreted fault slip periods. MC—Mechanic Creek gouge; BSG—Blue Sky porphyry breccia core gouge; BSC—Blue Sky porphyry breccia core carbonate; SC—Seymour Creek gouge; HC—Happy Creek gouge. (B) Fault dates linked to Big Creek fault slip periods with line drawings of Big Creek fault release bend and inferred rotated blocks. Blue arrows denote known or possible (?) presence of fluids during fault slip.

DISCUSSION

Fault Gouge

The MC and HC gouges, sampled close to the main fault trends, have very different host-rock ages (mid-Cretaceous and Paleozoic, respectively), yet have near-identical K-Ar results, with common ages of ca. 73 Ma and ca. 50 Ma (Fig. 2). BSPB and SC gouges, sampled from small fault zones situated within the fault bend blocks hosted by the same mid-Cretaceous granite as MC, yielded common ages of ca. 58 Ma and ca. 45 Ma (Fig. 2). Based on (1) a lack of primary igneous muscovite in wall rocks, (2) absence of other K-bearing phases in the dated fractions (except for minor traces of K-feldspar in the 2–0.6 µm fraction of HC gouge, which could explain its slightly older age of ca. 79 Ma), (3) clear disassociation between host-rock age and gouge illite K-Ar dates, and (4) illite morphology (Fig. 2), the dated illite samples are interpreted to reflect multiple fault-generated, authigenic illite ages with virtually no inherited component. The 2–0.6 µm fraction of SC gouge yielded a ca. 65 Ma age that was not reproduced in other size fractions or gouge samples. This lack of reproducibility suggests it represents a mixed age between older and ca. 58 Ma illite. For the above reasons, attempts to deconvolve the illite age results using the Illite Age Analysis method (Pevear, 1999), which assumes that different size fractions represent end-member mixtures of detrital grains and a single fault-gouge population, would be inappropriate for this study (e.g., Torgersen et al., 2015a).

All four samples yielded Eocene K-Ar ages for the <0.2 µm size fraction. This fine fraction could represent either late slip events, or partial thermal or fluid-related resetting that only affected the finest-grained illite. Thermal resetting of illite is possible above 260 ± 30 °C (Hunziker et al., 1986). Zircon (U-Th)/He ages from the study area are 79–70 Ma, indicating that the region was near or below ~180 °C, the nominal closure temperature for He in zircon, during all dated slip events (Bineli Betsi et al., 2012). Furthermore, apatite (U-Th)/He ages of 57–39 Ma show that the region was at ~60 °C or lower during the Eocene (Bineli Betsi et al., 2012). This rules out thermal resetting and suggests that the finest size fraction represents either two periods of illite growth during Eocene fault slip as implied in Figure 3, or growth during low-temperature fluid flow, or combined fault-fluid events.

Carbonate

Fault-related carbonate in the Big Creek fault releasing bend records ages of ca. 73 Ma and ca. 60–57 Ma (Table 1; Fig. 2). The Cretaceous U-Pb age is recorded in a carbonate vein, while both veins and slickenfibers record Paleocene ages. Thus, mineralized carbonate veining is associated with both periods of fault slip, consistent with mobilization of metals in carbonic fluids during syn- to post-mineralization faulting. The Cretaceous carbonate veins are not oriented parallel to the interpreted regional σ_1 (approximately north-south; Fig. 1E). Veins likely formed during crack-seal events along preferentially oriented (northeast-southwest) extensional fractures (Fig. 1E) parallel to a local σ_1 within rotated blocks in the fault bend (Fig. 3). These veins are parallel to regional northeast-trending faults (Fig. 1F; Sánchez et al., 2014). Subsequent <60 Ma fault slip and related fracturing and fluid flow reactivated preexisting (ca. 73 Ma) fractures during movement on the Big Creek fault, consistent with K-Ar illite results.

FAULT SLIP ON THE BIG CREEK FAULT

Fault slip periods at ca. 73 Ma and ca. 60–57 Ma interpreted from both the K-Ar illite and U-Pb carbonate results support Big Creek fault field relations indicating slip at 77–70 Ma and <70 Ma (Friend et al., 2017). Fault-gouge illite and carbonate record late– to post–granite emplacement fault movement at ca. 73 Ma (Fig. 3). Fault-gouge illite and carbonate slickenfibers and veins show subsequent reactivation at ca. 60–57 Ma along north-striking fault planes in the releasing bend at shallower crustal levels (Bineli Betsi et al., 2012; Fig. 3). This is compatible with minor offsets of ca. 72–67 Ma Carmacks Group volcanic rocks along the fault trace to the northwest (Colpron et al., 2016). Paleogene slip likely occurred throughout the northwest-southeast–trending dextral strike-slip fault corridor, coeval with the Tintina and Denali faults (Lanphere, 1978; Hayward, 2015; Sánchez et al., 2014), and also coincides with fault-related magmatism and mineralization in northern British Columbia (Ootes et al., 2017) and in the Canadian Rocky Mountains (Pană and van de Pluijm, 2015), suggesting the existence of a regionally extensive fault-controlled fluid-flow event. Subsequent slip at ca. 50 Ma (MC and HC gouge) and ca. 45 Ma (BSPB and SC gouge) can be inferred as continued reactivation as the Tintina and Denali faults continued to accommodate major displacements.

FAULTS AND FLUIDS

Our results provide, for the first time, an independent check on K-Ar illite and U-Pb carbonate direct fault dating methods. These methods provide complementary data sets, particularly useful toward resolving interpretational complexities arising from a fault history comprising multiple discrete faulting episodes. In the context of interpretation of K-Ar fault-gouge illite ages, our data corroborate previous work showing that different size fractions can record different slip periods (Torgersen et al., 2015a).

Because the age precision of our methods spans a few million years, the individual dates of fault-generated materials may span multiple seismic events during extended periods of fault activity. Furthermore, the study area records a complex faulting and fluid-flow history of which our data may represent only a partial history. However, the correspondence between field relationships and mineralized carbonate vein and fault-gouge illite ages contributes to understanding the interaction between faulting and fluid-flow periods. Although the carbonate veins formed coevally with seismic, gouge-generating fault slip periods, we do not have evidence for carbonate veins forming at other times in the absence of seismic slip. Within the constraints of our data set, the fault system may therefore have been impermeable during aseismic intervals. This implies empirical support for the fault-valve model, in which fluids are a major control on fault strength, and indicates that seismic pumping may have facilitated intervals of fluid flow (and hence mineralization) in this fault system (Sibson et al., 1975; Sibson, 1992). We anticipate that the ability to date multiple fault and fluid-related materials formed during fault slip events combined with chemical and stable-isotope methods will significantly advance future studies of fault-related fluid-rock systems.

ACKNOWLEDGMENTS

We acknowledge funding from the Geo-mapping for Energy and Minerals program of the Geological Survey of Canada and the U.K. Natural Environment Research Council (NERC) Arctic Office UK-Canada Bursary scheme. We gratefully acknowledge analytical and field assistance from M. Colpron, J. Powell, A. Grenier, I. Bilot, L. Bickerton, J. and E. Halle, G. Long, and J. Dunlop. We thank R. Parrish and R. Strachan for their feedback, and R. Holder, B. van der Pluijm, and an anonymous reviewer for constructive reviews. This is Natural Resources Canada publication #20200143.

REFERENCES CITED

Allan, M.M., and Friend, M., 2018, Bedrock geological map of the Mount Freegold district, Dawson Range (NTS 115I/6 and parts of 115I/2,3,5,7,10,11,12): Yukon Geological Survey Open File 2018-2, scale 1:50,000.

Allan, M.M., Mortensen, J.K., Hart, C.J.R., Bailey, L.A., Sánchez, M.G., Ciolkiewicz, W., McKenzie, G.G., and Creaser, R.A., 2013, Magmatic and metallogenic framework of west-central Yukon and eastern Alaska, *in* Colpron, M., et al., eds., Tectonics, Metallogeny, and Discovery: The North American Cordillera and Similar Accretionary Settings: Society of Economic Geologists Special Publication 17, p. 111–168, https://doi.org/10.5382/SP.17.04.

Ault, A.K., Reiners, P.W., Evans, J.P., and Thomson, S.N., 2015, Linking hematite (U-Th)/He dating with the microtextural record of seismicity in the Wasatch fault damage zone, Utah, USA: Geology, v. 43, p. 771–774, https://doi.org/10.1130/G36897.1.

Bineli Betsi, T., Lentz, D., McInnes, B., and Evans, N.J., 2012, Emplacement ages and exhumation rates for intrusion-hosted Cu-Mo-Sb-Au mineral systems at Freegold Mountain (Yukon, Canada): Assessment from U-Pb, Ar-Ar, and (U-Th)/He geochronometers: Canadian Journal of Earth Sciences, v. 49, no. 5, p. 653–670, https://doi.org/10.1139/e2012-009.

Colpron, M., Nelson, J.L., and Murphy, D.C., 2006, A tectonostratigraphic framework for the pericratonic terranes of the northern Canadian Cordillera, *in* Colpron, M., and Nelson, J.L., eds., Paleozoic Evolution and Metallogeny of Pericratonic Terranes and the Ancient Pacific Margin of North America, Canadian and Alaskan Cordillera: Geological Association of Canada Special Paper 45, p. 1–23.

Colpron, M., Isreal, S., Murphy, D., Pigage, L., and Moynihan, D., 2016, Yukon bedrock geology map: Yukon Geological Survey Open File 2016-1, scale 1:1,000,000.

Friend, M.A., Allan, M.M., and Hart, C.J.R., 2017, New contributions to the bedrock geology of the Mount Freegold district, Dawson Range, Yukon (NTS 115I/2, 6 and 7), *in* MacFarlane, K.E., ed., Yukon Exploration and Geology 2017: Whitehorse, Yukon Geological Survey, p. 47–68.

Haines, S., Lynch, E., Mulch, A., Valley, J.W., and van der Pluijm, B., 2016, Meteoric fluid infiltration in crustal-scale normal fault systems as indicated by $\delta^{18}O$ and $\delta^{2}H$ geochemistry and $^{40}Ar/^{39}Ar$ dating of neoformed clays in brittle fault rocks: Lithosphere, v. 8, p. 587–600, https://doi.org/10.1130/L483.1.

Hayward, N., 2015, Geophysical investigation and reconstruction of lithospheric structure and its control on geology, structure, and mineralization in the Cordillera of northern Canada and eastern Alaska: Tectonics, v. 34, p. 2165–2189, https://doi.org/10.1002/2015TC003871.

Hunziker, J.C., Frey, M., Clauer, N., Dallmeyer, R.D., Friedrichsen, H., Flehmig, W., Hochstrasser, K., Roggwiler, P., and Schwander, H., 1986, The evolution of illite to muscovite: Mineralogical and isotopic data from the Glarus Alps, Switzerland: Contributions to Mineralogy and Petrology, v. 92, p. 157–180, https://doi.org/10.1007/BF00375291.

Johnston, S.T., 1999, Large-scale coast-parallel displacements in the Cordillera: A granitic resolution to a paleomagnetic dilemma: Journal of Structural Geology, v. 21, p. 1103–1108, https://doi.org/10.1016/S0191-8141(99)00015-2.

Lanphere, M.A., 1978, Displacement history of the Denali fault system, Alaska and Canada: Canadian Journal of Earth Sciences, v. 15, p. 817–822, https://doi.org/10.1139/e78-086.

Nuriel, P., Rosenbaum, G., Zhao, J.-X., Feng, Y., Golding, S.D., Villemant, B., and Weinberger, R., 2012, U-Th dating of striated fault planes: Geology, v. 40, p. 647–650, https://doi.org/10.1130/G32970.1.

Nuriel, P., Weinberger, R., Kylander-Clark, A.R.C., Hacker, B.R., and Craddock, J.P., 2017, The onset of the Dead Sea transform based on carbonate age-strain analyses: Geology, v. 45, p. 587–590, https://doi.org/10.1130/G38903.1.

Nuriel, P., Miller, D.M., Schmidt, K.M., Coble, M.A., and Maher, K., 2019a, Ten-million years of activity within the Eastern California Shear Zone from U-Pb dating of fault-zone opal: Earth and Planetary Science Letters, v. 521, p. 37–45, https://doi.org/10.1016/j.epsl.2019.05.047.

Nuriel, P., Craddock, J., Kylander-Clark, A.R.C., Uysal, I.T., Karabacak, V., Dirik, R.K., Hacker, B.R., and Weinberger, R., 2019b, Reactivation history of the North Anatolian fault zone based on carbonate age-strain analyses: Geology, v. 47, p. 465–469, https://doi.org/10.1130/G45727.1.

Ootes, L., Elliott, J.M., and Rowins, S.M., 2017, Testing the relationship between the Llewellyn fault, gold mineralization, and Eocene volcanism in northwest British Columbia: A preliminary report, *in* Geological Fieldwork 2016, British Columbia Ministry of Energy and Mines, British Columbia Geological Survey Paper 2017-1, p. 49–59.

Pană, D.I., and van der Pluijm, B.A., 2015, Orogenic pulses in the Alberta Rocky Mountains: Radiometric dating of major faults and comparison with the regional tectono-stratigraphic record: Geological Society of America Bulletin, v. 127, p. 480–502, https://doi.org/10.1130/B31069.1.

Parrish, R.R., Parrish, C.M., and Lasalle, S., 2018, Vein calcite dating reveals Pyrenean orogen as cause of Paleogene deformation in southern England: Journal of the Geological Society, v. 175, p. 425–442, https://doi.org/10.1144/jgs2017-107.

Pevear, D.R., 1999, Illite and hydrocarbon exploration: Proceedings of the National Academy of Sciences of the United States of America, v. 96, p. 3440–3446, https://doi.org/10.1073/pnas.96.7.3440.

Rasbury, E.T., and Cole, J.M., 2009, Directly dating geologic events: U-Pb dating of carbonates: Reviews of Geophysics, v. 47, RG3001, https://doi.org/10.1029/2007RG000246.

Roberts, N.M., and Walker, R.J., 2016, U-Pb geochronology of carbonate-mineralized faults: Absolute timing of rift-related fault events on the northeast Atlantic margin: Geology, v. 44, p.531–534, https://doi.org/10.1130/G37868.1.

Roberts, N.M.W., et al., 2020, Laser ablation inductively coupled plasma mass spectrometry (LA-ICP-MS) U-Pb carbonate geochronology: Strategies, progress, and limitations: Geochronology, v. 2, p. 33–61, https://doi.org/10.5194/gchron-2-33-2020.

Sánchez, M.G., Allan, M.M., Hart, C.J., and Mortensen, J.K., 2014, Extracting ore-deposit-controlling structures from aeromagnetic, gravimetric, topographic, and regional geologic data in western Yukon and eastern Alaska: Interpretation (Tulsa), v. 2, no. 4, p. SJ75–SJ102, https://doi.org/10.1190/INT-2014-0104.1.

Sibson, R.H., 1992, Implications of fault-valve behaviour for rupture nucleation and recurrence: Tectonophysics, v. 211, p. 283–293, https://doi.org/10.1016/0040-1951(92)90065-E.

Sibson, R.H., Moore, J.M.M., and Rankin, A.H., 1975, Seismic pumping—A hydrothermal fluid transport mechanism: Journal of the Geological Society, v. 131, p. 653–659, https://doi.org/10.1144/gsjgs.131.6.0653.

Tagami, T., 2012, Thermochronological investigation of fault zones: Tectonophysics, v. 538, p. 67–85, https://doi.org/10.1016/j.tecto.2012.01.032.

Tillberg, M., Drake, H., Zack, T., Kooijman, E., Whitehouse, M.J., and Åström, M.E., 2020, *In situ* Rb-Sr dating of slickenfibres in deep crystalline basement faults: Scientific Reports, v. 10, 562, https://doi.org/10.1038/s41598-019-57262-5.

Torgersen, E., Viola, G., Zwingmann, H., and Henderson, I.H.C., 2015a, Inclined K-Ar illite age spectra in brittle fault gouges: Effects of fault reactivation and wall-rock contamination: Terra Nova, v. 27, p. 106–113, https://doi.org/10.1111/ter.12136.

Torgersen, E., Viola, G., Zwingmann, H., and Harris, C., 2015b, Structural and temporal evolution of a reactivated brittle-ductile fault—Part II: Timing of fault initiation and reactivation by K-Ar dating of synkinematic illite/muscovite: Earth and Planetary Science Letters, v. 410, p. 212–224, https://doi.org/10.1016/j.epsl.2014.09.051.

Tsukamoto, S., Tagami, T., and Zwingmann, H., 2019, Direct dating of fault movement, *in* Tanner, D., and Brandes, C., eds., Understanding Faults: Detecting, Dating, and Modeling: Amsterdam, Elsevier, p. 257–283, https://doi.org/10.1016/B978-0-12-815985-9.00007-2.

van der Pluijm, B.A., Hall, C.M., Vrolijk, P.J., Pevear, D.R., and Covey, M.C., 2001, The dating of shallow faults in the Earth's crust: Nature, v. 412, p. 172–175, https://doi.org/10.1038/35084053.

Vrolijk, P., Pevear, D., Covey, M., and LaRiviere, A., 2018, Fault gouge dating: History and evolution: Clay Minerals, v. 53, p. 305–324, https://doi.org/10.1180/clm.2018.22.

Zwingmann, H., and Mancktelow, N., 2004, Timing of Alpine fault gouges: Earth and Planetary Science Letters, v. 223, p. 415–425, https://doi.org/10.1016/j.epsl.2004.04.041.

Zwingmann, H., Yamada, K., and Tagami, T., 2010, Timing of brittle deformation within the Nojima fault zone, Japan: Chemical Geology, v. 275, p. 176–185, https://doi.org/10.1016/j.chemgeo.2010.05.006.

Printed in USA